

Supplementary Material

1 **Discorhabdin N, a South African natural
2 compound, for Hsp72 and Hsc70 allosteric
3 modulation: Combined study of molecular
4 modeling and dynamic residue network
5 analysis**

6 **Arnold Amusengeri^{1a} and Özlem Tastan Bishop^{1b*}**

7 ¹Research Unit in Bioinformatics (RUBi), Department of Biochemistry and Microbiology,
8 Rhodes University, Grahamstown, 6140, South Africa

9 *** Correspondence:**

10 Özlem Tastan Bishop

11 email: O.TastanBishop@ru.ac.za

12

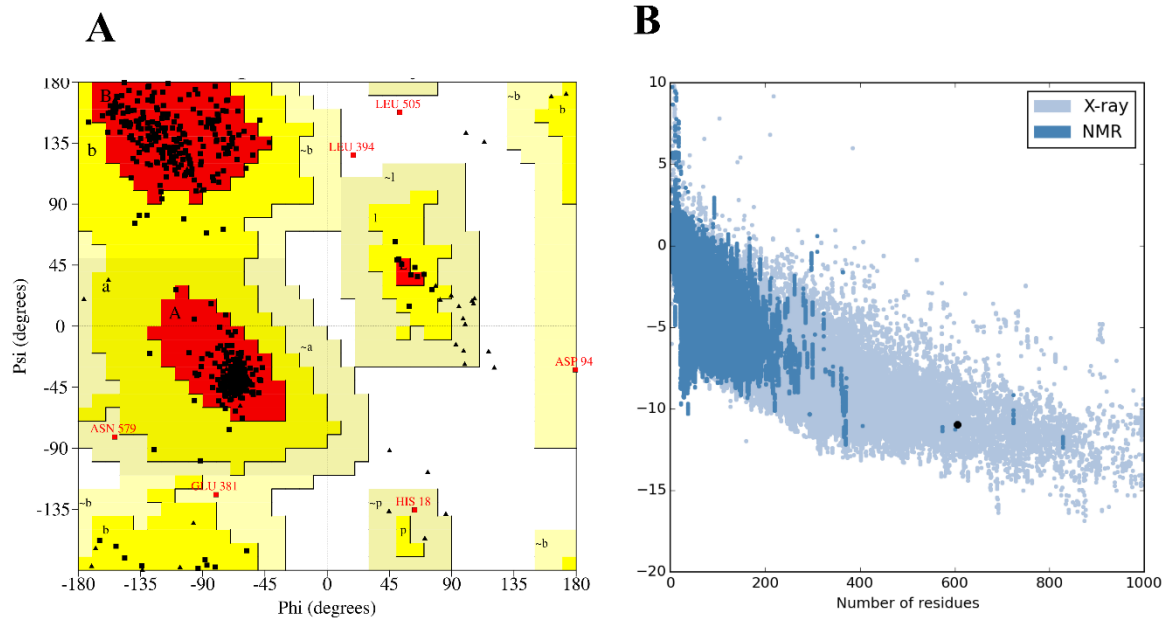
13 **Table S1: Structure validation results:** Tabulated summary of Z-dope, Ramachandran,
14 ProSA and Verify-3D results.

15

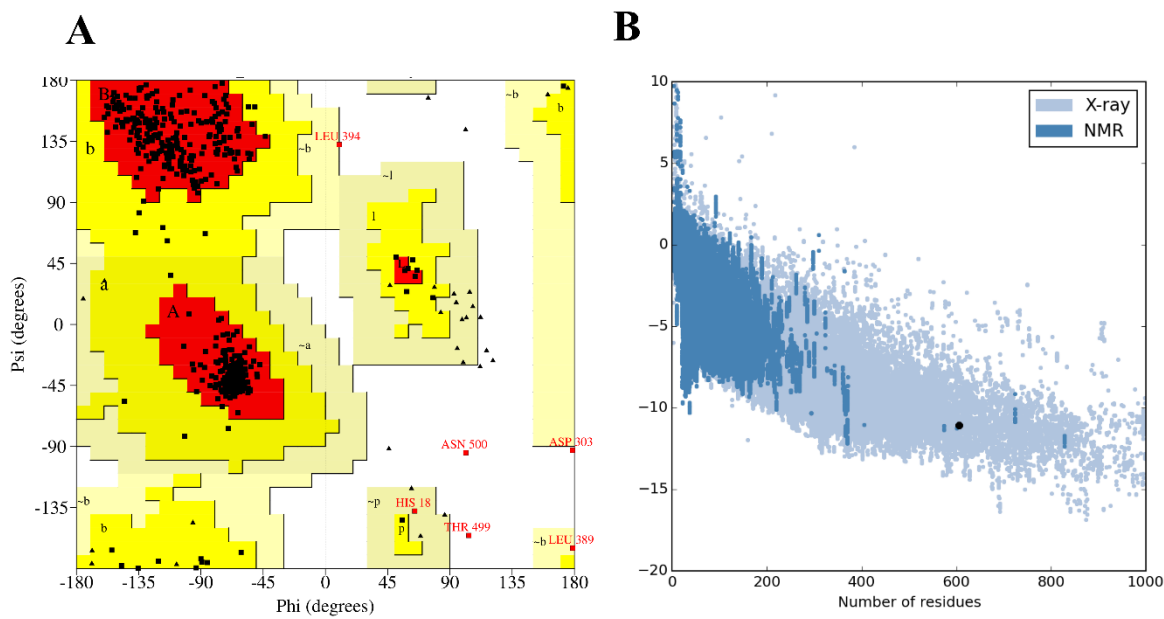
Protein	Z-Dope score	PROCHECK (Ramachandran Plot)				ProSA Z-Score	Verify 3D	
		Number of residues in favoured region (Percentage value)	Number of residues in additional allowed region (Percentage value)	Number of residues in generously allowed region (Percentage value)	Number of residues in disallowed region (Percentage value)		Score	Comment
Hsp72	-0.51	93.70%	5.20%	0.70%	0.40%	-10.98	85.81%	Pass
Hsc70	-0.56	94.10%	4.80%	0.50%	0.50%	-11.07	83.99%	Pass

16

Hsp72



Hsc70

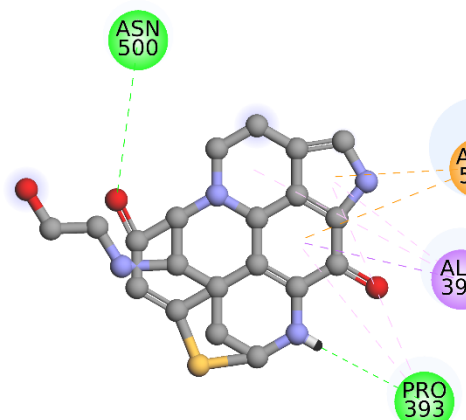


17

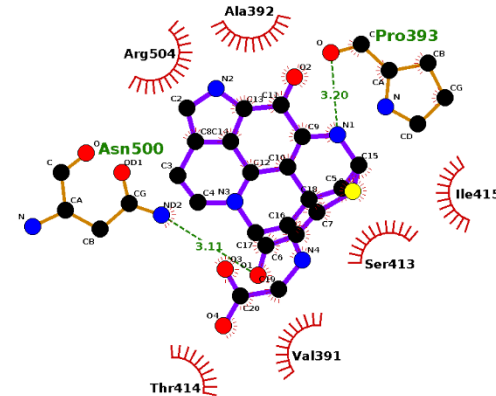
18 **Figure S1: Model validation summary.** (A) **Ramachandran plots.** In both proteins, more
 19 than 90% of all residues occupied the most favoured region (Hsp72: 93.70%, Hsc70:
 20 94.10%). (B) **ProSA results.** Both proteins recorded low Z-Score values (Hsp72: -10.98,
 21 Hsc70: -11.07) that were within the range of high resolution crystallized proteins.

Hsp72

A



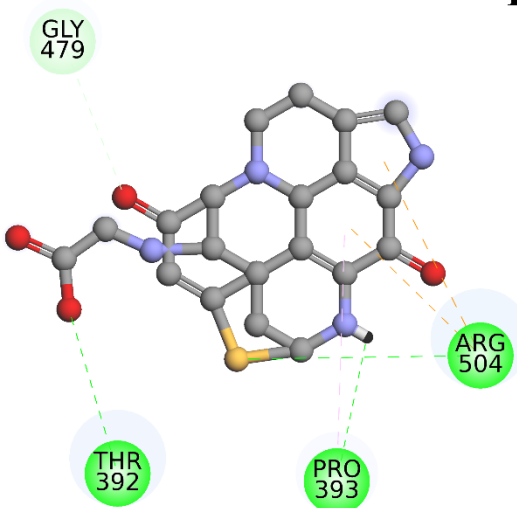
B



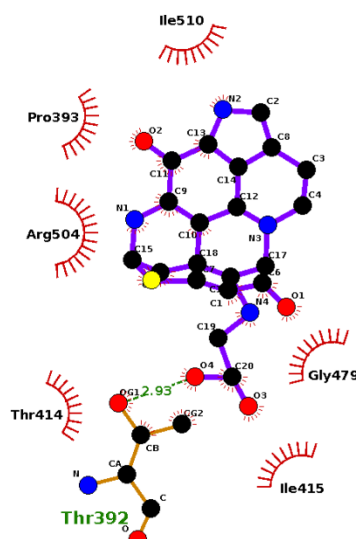
Hsp72_SANC00132

Hsc70

A



B



Hsc70-SANC00132

22

23 **Figure S2: Molecular docking interactions visualised using (A) Discovery studio**
 24 **visualizer, and (B) LigPlot+.** (A) SANC00132 is displayed in ball and stick while non-
 25 bonded interactions are shown as dashed lines. (B) SANC00132 is represented in ball and
 26 stick while bonds are shown sticks (purple solid lines). Hydrogen bonds are shown as dashed
 27 green lines while protein residues making hydrogen bond connections are represented in ball
 28 and stick.

29 **Table S2: Tabulated results from Vina and XScore scoring tools.**

30

Compound	Molecular weight (g/mol)	Protein	Vina		X-Score				
			Vina Score (Kcal/mol)	Rank	HPScore (pKd)	HMScore (pKd)	HSScore (pKd)	Average (pKd)	Rank
SANC00132	396.30	Hsp72	-6.9	7	5.56	5.48	5.48	5.51	14
		Hsc70	-7.1	11	5.78	5.91	5.53	5.74	5

31

32 **Table S3: Post-docking analysis results.** Tabulated results of (A) Hsp72 and (B) Hsc70
33 residues interacting with SANC00132.

34

35 (A)

Hsp72	
Hsp72 interacting residues (DNAK numbering)	Hsp72 complete sequence equivalent
ALA392	ALA397
PRO393	PRO398
ASN500	ASN505
ARG504	ARG509

36

37 (B)

Hsc70	
Hsc70 interacting residues (DNAK numbering)	Hsc70 complete sequence equivalent
THR392	THR397
PRO393	PRO398
GLY479	GLY484
ARG504	ARG509

38

39 **Table S4: Results of computed molecular descriptors using FAF-Drugs4 web-server.**
 40 SANC00132 passed the Lipinski tests for drug likeness (RO5) including Molecular mass <
 41 500 Dalton: MW = 410.45, Lipophilicity (LogP) < 5: logP = -2.36, Hydrogen bond donors <
 42 5: HBD = 4, and Hydrogen bond acceptors < 10: HBA = 8.

43

Ligand	SANC00132
MW	410.45
logP	-2.36
logD	-3.76
logSw	-0.78
tPSA	147.24
RotatableB	3
RigidB	31
Flexibility	0.09
HBD	4
HBA	8
HBD_HBA	12
Rings	1
MaxSizeRing	24
NumCharges	2
TotalCharge	0
HeavyAtoms	29
CarbonAtoms	20
HeteroAtoms	9
ratioH/C	0.45
Lipinski_Violation	0
Solubility(mg/l)	188397.59
SolubilityForecastIndex	Good Solubility
Oral_Bioavailability_VEBER	Good
Oral_Bioavailability_EGAN	Good
TrafficLights	3
4_400	good
3_75	good
Phospholipidosis	NonInducer
Fsp3	0.45
StereoCenters	5
PAINS_Filter_A	0
PAINS_Filter_B	0
PAINS_Filter_C	0
Result	Accepted

44

45 **Table S5:** Tabulated RMSD convergence values

46

Protein	RMSD convergence value	
Hsp72 apo run1	Run1	~1.5 nm
	Run2	~1.2 nm
Hsp72 endo-apo	Run1	~1.2 nm
	Run2	~1.9 nm
Hsc70 apo	Run1	~1.5 nm
	Run2	~1.7 nm
Hsc70 endo-apo	Run1	~1.6 nm
	Run2	~1.3 nm
Hsp72-SANC00132 complex	Run1	~1.5 nm
	Run2	~1.5 nm
Hsp72 endo-complex	Run1	~0.7 nm
	Run2	~1.5 nm
Hsc70-SANC00132 complex	Run1	~1.2 nm
	Run2	~1.2 nm
Hsc70 endo-complex	Run1	~1.5 nm
	Run2	~1.5 nm

47

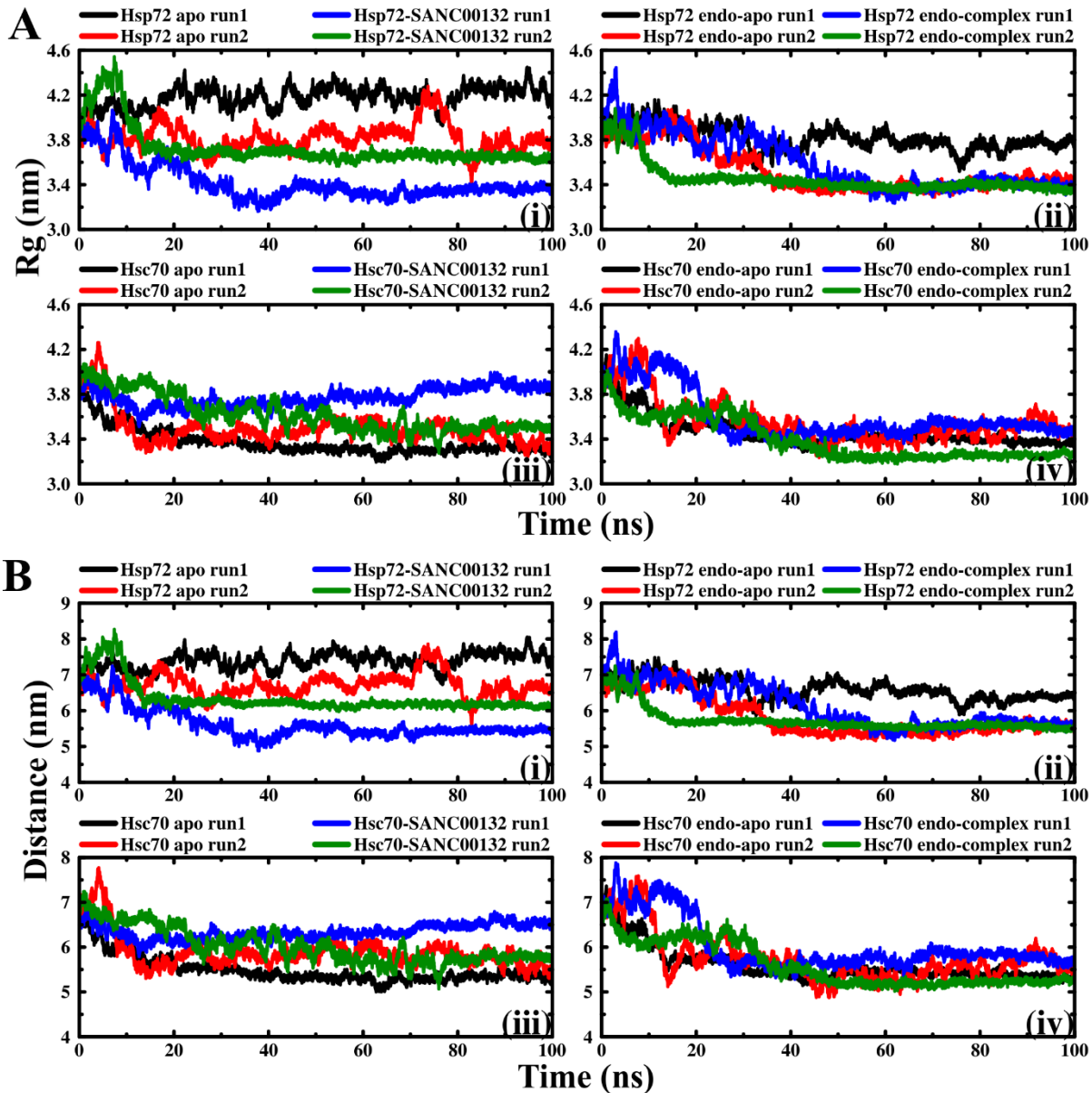


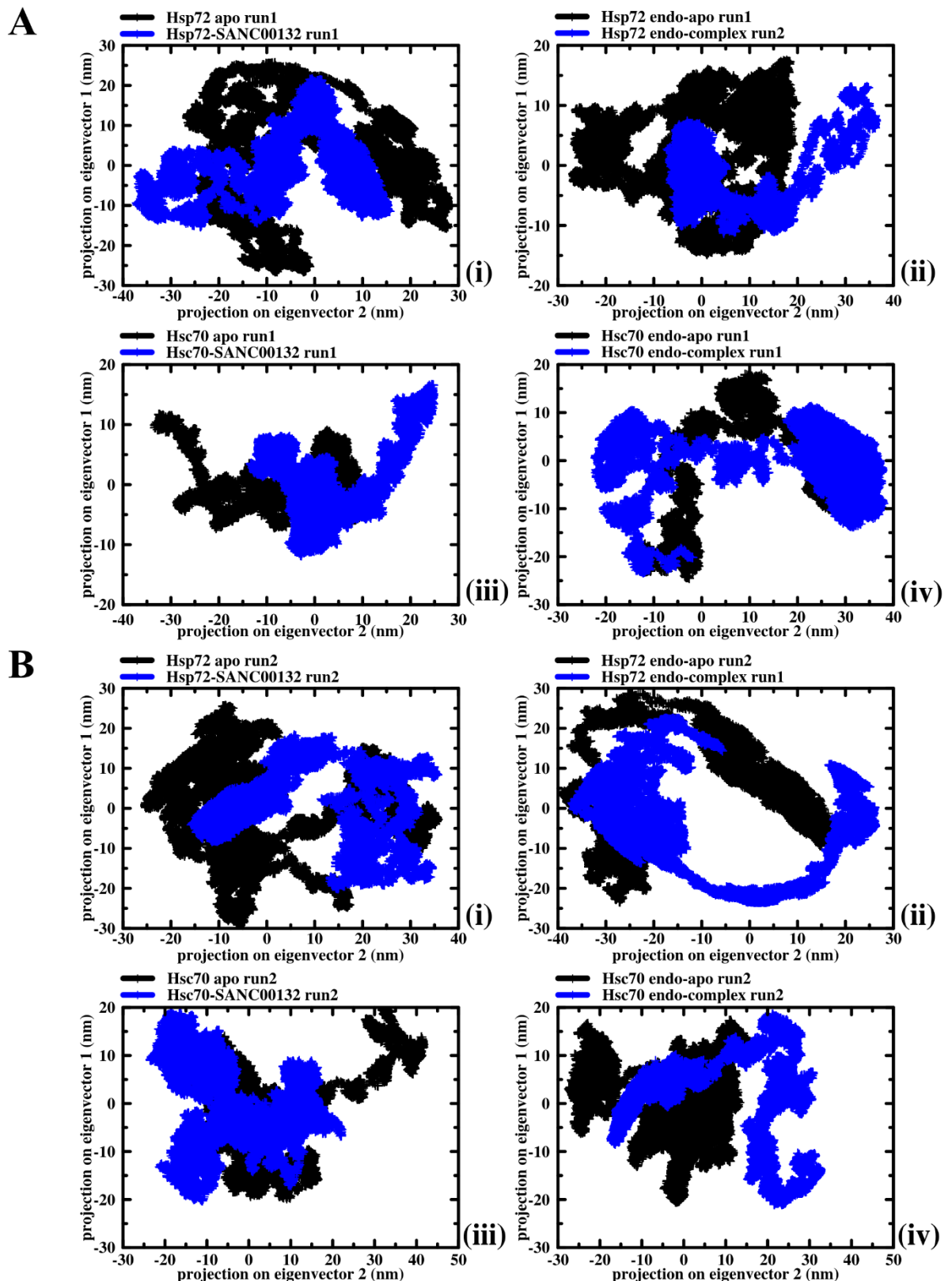
Figure S3: (A) Time dependent radius of gyration (R_g) of Hsp72 and Hsc70 during 100ns simulation. (i) Hsp72 Set1, (ii) Hsp72 Set2, (iii) Hsc70 Set1, (iv) Hsc70 Set2. (B) Time-dependent distance between the centre of mass of the NBD and that of the SBD. (i) Hsp72 Set1, (ii) Hsp72 Set2, (iii) Hsc70 Set1, (iv) Hsc70 Set2. Colour code: Black and red: inhibitor-free, Blue and green: inhibitor-bound.

55 **Table S6: Tabulated values of the percentage variance contributed by the first two**
 56 **principal components. Also displayed are respective trace values of diagonalized**
 57 **covariance matrices of each MD trajectory.**

58

Protein systems		Percentage variance accounted by each component		Trace value / cumulative sum of eigenvalues (nm ²)	Trace value variance between Run1 and Run2
		PC1 (%)	PC2 (%)		
Hsp72 apo	Run1	54.10	24.96	520.860	3854.51
	Run2	55.12	27.31	433.059	
Hsp72-SANC00132 complex	Run1	57.54	24.03	263.135	353.89
	Run2	63.10	16.64	236.531	
Hsp72 endo-apo	Run1	46.01	23.76	247.669	15335.08
	Run2	70.88	19.48	422.798	
Hsp72 endo-complex	Run1	70.06	18.35	635.812	1522120.50
	Run2	62.00	13.95	84.2316	
Hsc70 apo	Run1	71.04	8.80	99.7293	5550.44
	Run2	48.94	29.23	205.09	
Hsc70-SANC00132 complex	Run1	47.79	21.59	129.313	4895.25
	Run2	58.47	26.04	228.26	
Hsc70 endo-apo	Run1	59.96	27.82	209.165	65.38
	Run2	42.19	22.91	197.73	
Hsc70 endo-complex	Run1	78.62	9.45	350.493	37.27
	Run2	75.85	13.66	341.859	
					Total variance =182212.3
					Average standard deviation ($\sqrt{(\text{Total variance})}$) = 426.86

59

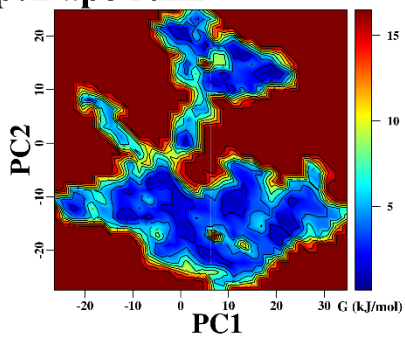


60

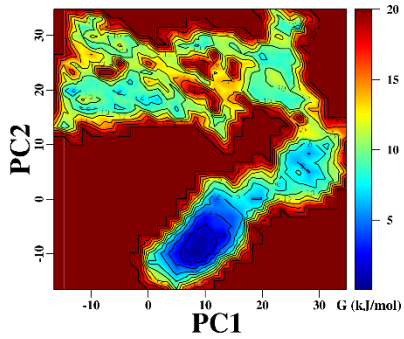
61 **Figure S4: 2D projection of first and second principal components.** Colour key: Black:
62 inhibitor-free, Blue; inhibitor-bound. **A:** Initial simulations, **B:** Duplicate simulations.

63

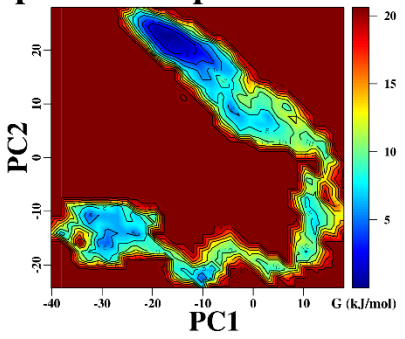
A (i) Hsp72 apo run2



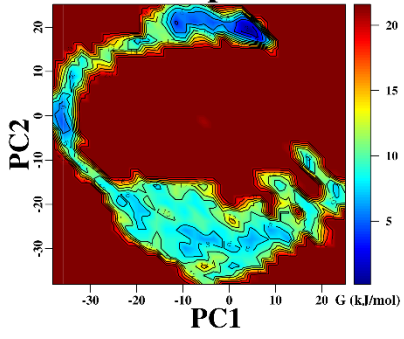
(ii) Hsp72 SANC00132 run2



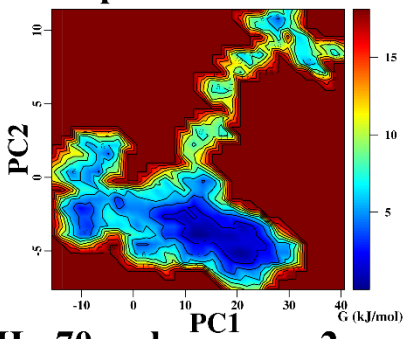
(iii) Hsp72 endo-apo run2



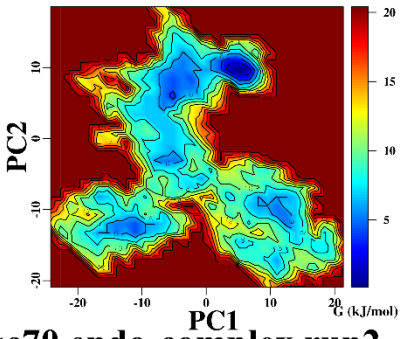
(iv) Hsp72 endo-complex run1



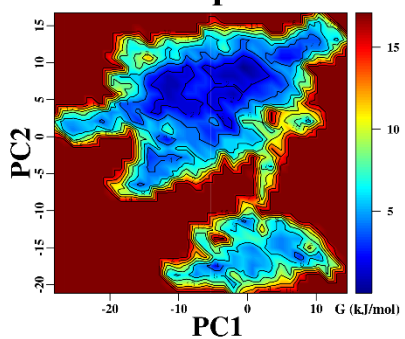
B (i) Hsc70 apo run2



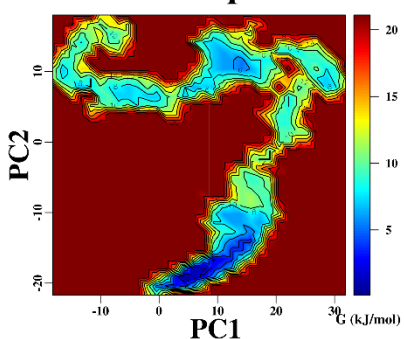
(ii) Hsc70 SANC00132 run2



(iii) Hsc70 endo-apo run2



(iv) Hsc70 endo-complex run2



64

65 **Figure S5: Free energy landscape projections along the first and second principal**
66 **components. A: Hsp72: (i) Hsp72 apo Run2, (ii) Hsp72-SANC00132 Run2, (iii) Hsp72**
67 **endo-apo Run2 (iv) Hsp72 endo-complex Run1. B: Hsc70: (i) Hsc70 apo Run2,**
68 **(ii) Hsc70 SANC00132 Run2, (iii) Hsc70 endo-apo Run2 (iv) Hsc70 endo-complex Run2.**

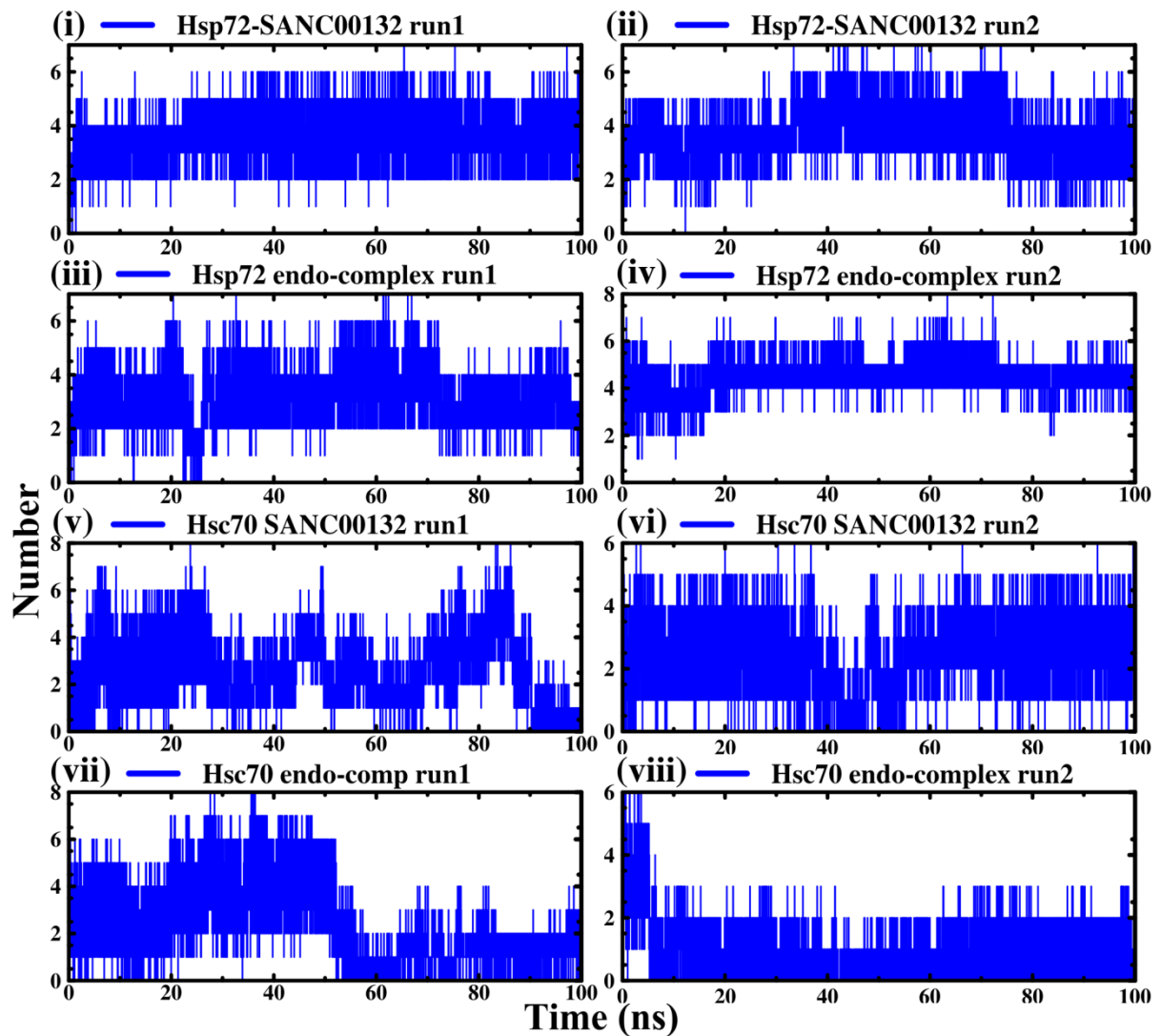
69

70 **Table S7: Per residue contribution to the total binding free energy.** Residues contributing
 71 $> \pm 5 \text{ kJmol}^{-1}$ of the total binding free energy were summarised below.

72

Protein-ligand complex		Per residue contribution to total BFE		Standard deviation
		Residue	Binding energy (kJmol^{-1})	
Hsp72-SANC00132 complex	Run1	ALA392	-9.2929	0.8923083
		PRO393	-5.6193	
		ILE415	-8.5837	
		GLU439	9.6769	
		ARG504	-5.7884	
	Run2	VAL391	-5.2542	0.8634035
		LEU396	-11.3954	
		ILE415	-8.3079	
		GLU439	-5.9290	
		ILE475	-5.8271	
Hsp72 endo-complex	Run1	ALA392	-7.0066	
		ILE415	-9.7801	
	Run2	ARG166	7.0044	1.041394
		ASP390	10.5007	
		VAL391	-6.7432	
		ALA392	-6.6763	
		LEU394	-6.2393	
		LEU396	-10.4549	
		THR414	-5.7496	
		GLU439	6.9388	
Hsc70-SANC00132 complex	Run1	LEU481	-6.0443	0.977574
		Val391	-8.4813	
		ASP501	-6.7608	
		ARG504	10.7052	
	Run2	LYS507	14.0571	0.6952183
		PRO393	-9.4854	
Hsc70 endo-complex run1	Run1	ILE415	-7.7102	0.9081865
		HIS18	-8.9954	
		GLY19	-5.0711	
		LEU386	-5.1133	
		VAL391	-11.1632	
		GLU439	-5.1557	
	Run2	GLY479	-5.4216	0.8594879
		ARG504	9.8270	
		THR392	-10.0733	
		GLY479	-6.1143	

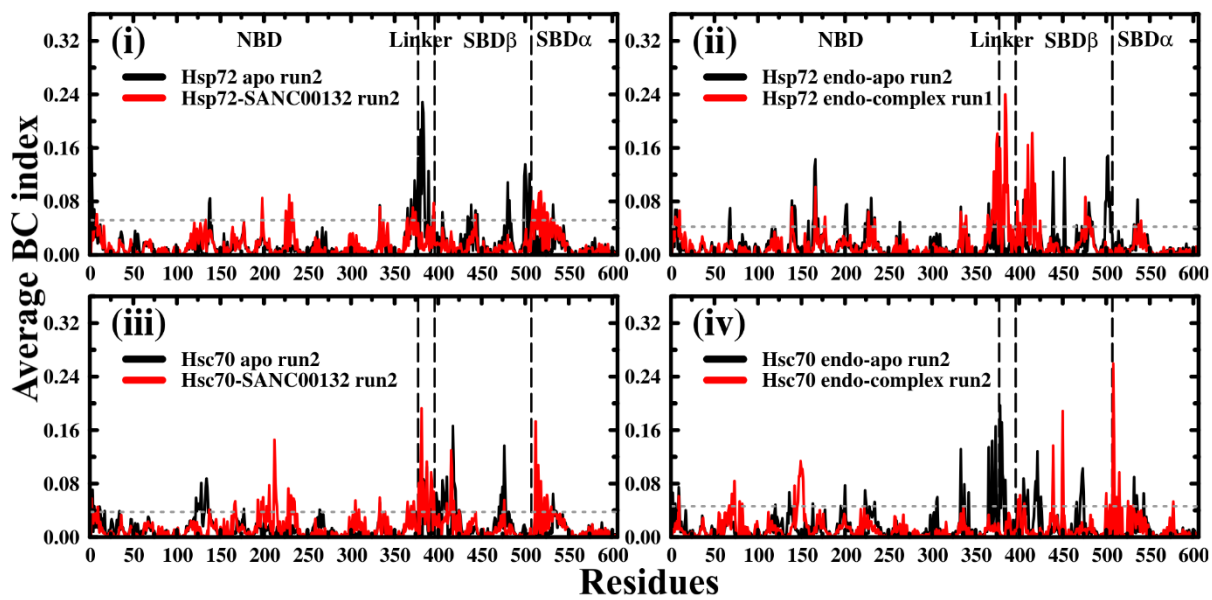
73



74

75 **Figure S6: Plots showing the number of hydrogen bonds formed between protein-ligand**
 76 **complexes throughout the simulation period.**

77



78

79 **Figure S7: Contact network analysis: Betweenness centrality results for duplicate**
80 **simulations.** The lower threshold values of 0.05 (Hsp72 apo run2), 0.04 (Hsp72 endo-apo

81 run2), 0.04 (Hsc70 apo run2), and 0.05 (Hsc70 endo-apo run2) are indicated by the dotted
82 grey lines.

83 **Table S8: Tabulated summary of residues having low average (L) values.** Equivalent
84 residue numbering from complete Hsp72 and Hsc70 sequences (accession numbers
85 NP_005337.2 and AAK17898.1 respectively). **(A and B)** Inhibitor free and inhibitor-bound
86 protein residues translated from **Table 1**.

87 **(A) Inhibitor-free proteins**

Protein	Residues
Hsp72	ALA6-THR14, CYY17 - GLN19, GLU27 – ILE29, TYR41, ARG72, LEU124, THR125, GLU132, THR140, ALA142-TYR149, GLN156, LYS159, ASP160, VAL163, ASN168-LEU185, PHE198-LEU200, LEU336, GLY338, ASN364, ASP366, ALA368-GLN389
Hsc70	ALA6-GLN22, GLU27, ILE29, ALA30, PRO39, TYR41, ARG72, GLY75, SER121, MET122, LEU124, THR125, MET127-GLU129, ALA131, GLU132, THR140-ASN151, LYS159-THR163, GLY166-TYR183, GLY338, ALA368-GLY382, GLN389

88

89 **(B) Inhibitor-bound proteins**

Protein	Residues
Hsp72	GLY8-THR13, CYS17-VAL20, GLU25, ILE29, VAL133-TYR149, ILE172-ARG187, LEU196-LEU200, ILE209-THR211, GLU218, LEU334-GLY339, ARG342, LYS361, ASN364-ILE379, MET381, ASP395, ILE420-LYS423, ASP481, ASN483-ILE485
Hsc70	ALA6-THR14, CYS17-PHE21, ILE29, TYR41, LYS71, ARG72, ARG76, SER121, LEU124, THR125, LYS128, GLU129, GLU132, ALA142-TYR149, ASN151, ARG155, GLU156, LYS159, ASP160, GLY162, THR163, GLY166, ASN168-TYR183, PHE198, LEU200, ILE209, THR211, LYS221, ALA368-ILE379, SER381, GLY382, LEU391

90

91 **Table S9: Residues that yielded high betweenness values: Corresponding residue**
 92 **numbering from complete Hsp72 and Hsc70 sequences (accession numbers**
 93 **NP_005337.2 and AAK17898.1 respectively). (A and B) Residues from inhibitor-free**
 94 **proteins and inhibitor-bound proteins translated from Table 3.**

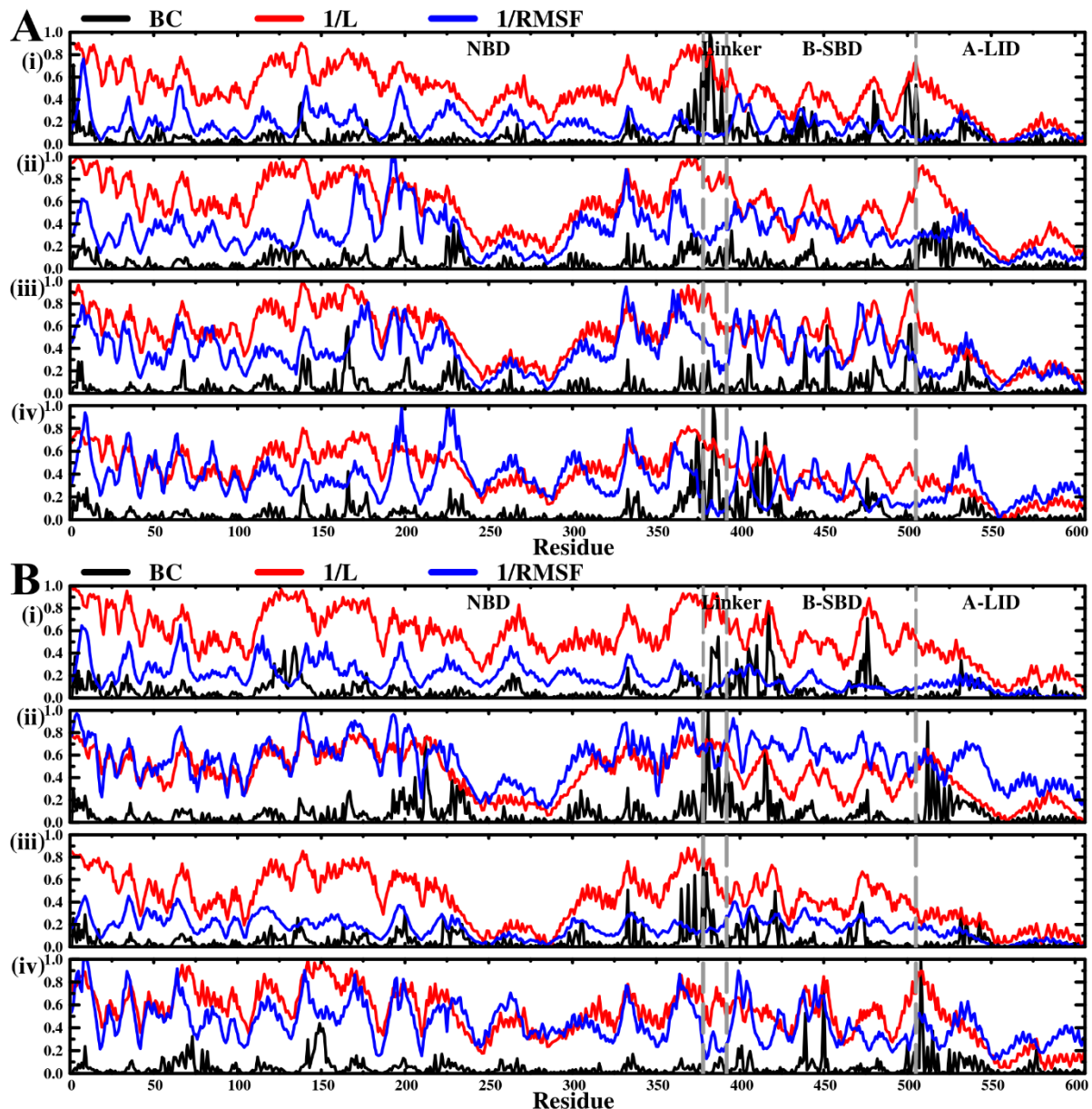
95

96 **(A) Inhibitor-free proteins**

Protein	Residues
Hsp72	ILE7, ASP10, GLY12, VAL143, ILE144, LEU170, ARG171, ASN174, ALA182, ASP206, GLU231, ASN235, ASN239, GLY338, ARG342, ALA370, ALA374, ALA377-ILE379, SER381-ASP395, LEU399, SER400, THR410, THR411, TYR443, GLU444, GLU446, ALA448, GLY457, ILE485, ASN487, THR489, THR504-LYS507, ARG509-LEU510, GLU516, SER537, ASN540, ALA541
Hsc70	VAL7, GLY8, ASP10-GLY12, THR14, CYS17, TYR41, LYS88, TRP90, LYS102, PRO116, SER121, LEU124, THR125, MET127, LYS128, ALA133, VAL139, ASN141, VAL143-VAL146, ILE164, ASN174, PRO176, ALA182, LYS188, LEU200, PHE205, LEU228, ASP234, ASN235, ASN239, ALA270, GLY338, ARG342, GLN347, VAL369, ALA370, ALA374, GLN376-ALA378, ASP383, SER385-GLU386, VAL388-LEU392, ILE403, GLU404, ALA406, MET410-VAL412, ILE414, LYS415, THR422-GLN426, THR429, THR430, MET449, GLY459, GLY470, VAL471, GLU475, THR477-ASP479, ASP481, ALA482, LEU486-SER489, THR504-ASP506, ARG509, SER542, ASN540, SER541, TYR545, ASN548, MET549, ASP582

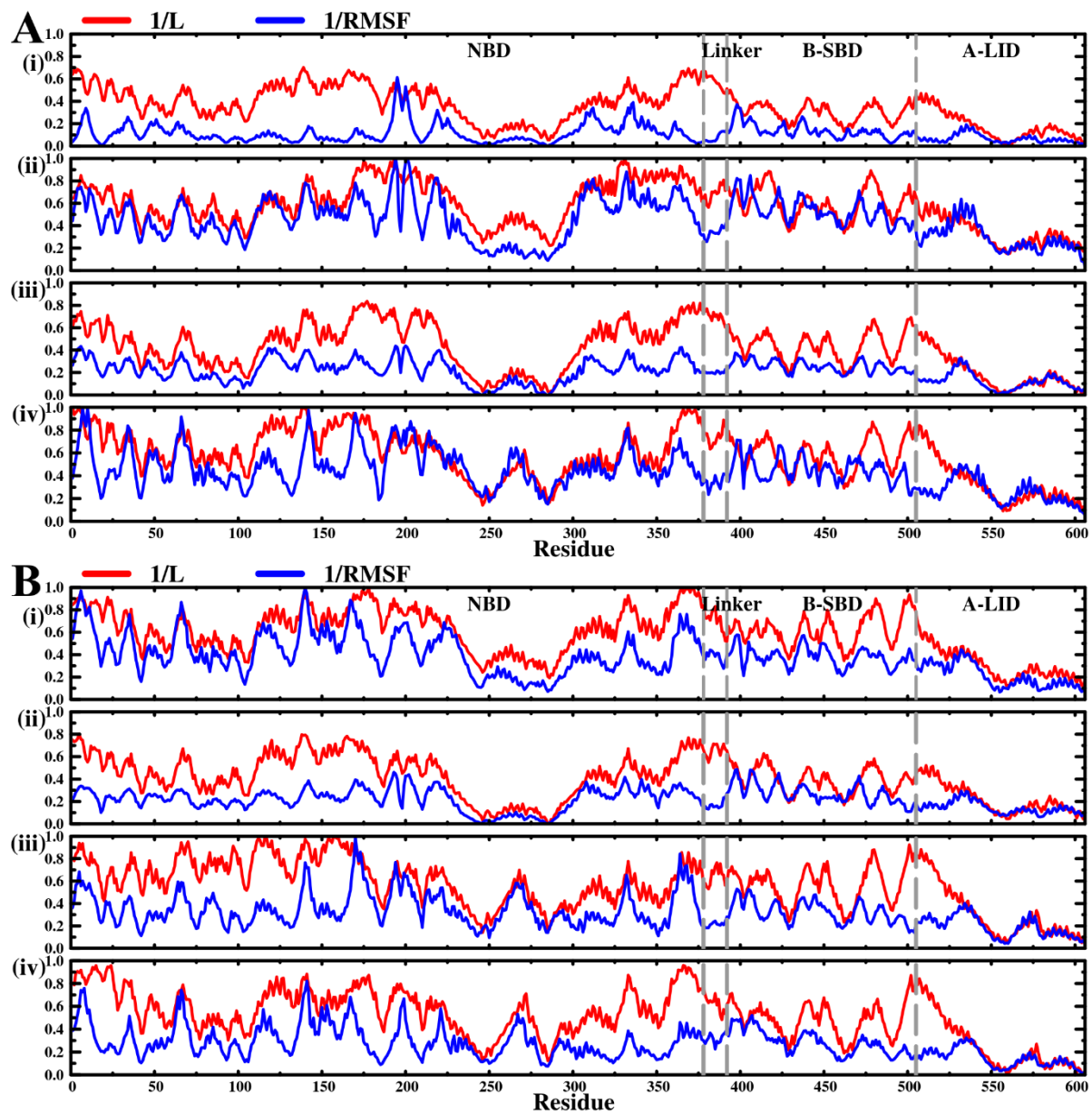
97 **(B) Inhibitor-bound proteins**

Protein	Residues
Hsp72	ASP10-CYS17, LEU124, THR125, GLU132, VAL143, ILE144, VAL146, ARG171, ASN174, ALA179-TYR183, LEU196, GLY203, GLU231, ASP234, ASN235, VAL238, ASN239, LEU336, GLY338, ARG342, PRO344, GLN347, VAL369, ALA370, GLY372, ALA374 - LEU380, GLY382, ASP383, ASN387, GLN389-LEU392, ASP395, SER400, LEU403, ALA406, MET410-LEU413, LYS415, THR419-PRO421, LYS423, THR429, THR429, GLN441, ALA448, THR479, ASP481, GLY484, ILE485, LEU486, VAL488, THR489, THR504, ASP506, LYS512, GLU516, GLN520, GLU523, ALA527, SER537, ALA538, ALA541, LEU542, TYR545, MET549
Hsc70	ASP10, GLY12, THR14, TYR15, VAL18, GLU27 - ILE29, ARG72, ARG76, LEU124, THR125, VAL143 - PRO147, PHE150, GLN154 - GLN156, ASN168, VAL169, ARG171, ASN174, PRO176, LEU200, GLY202, THR204, ASP206, THR211, PHE217, GLU218, GLY229, PHE233, ARG236, ASN239, PHE310, GLY338, ARG342, VAL369, ALA370, GLY372, ALA374, ALA377, ASP383, GLU386, VAL388, ASP390, LEU391, LEU392, ASP395 - PRO398, SER400, ILE403, GLU404, ALA406, MET410 - VAL412, LYS415, THR419 - PRO421, GLN441, GLU444, ALA448, LEU455, ASN487, ASN505, LYS507, SER511 - ASP514, GLU516, ARG517, GLN520, GLU523, GLU530, SER537, SER538, ASN540 - TYR545, MET549, ASP582

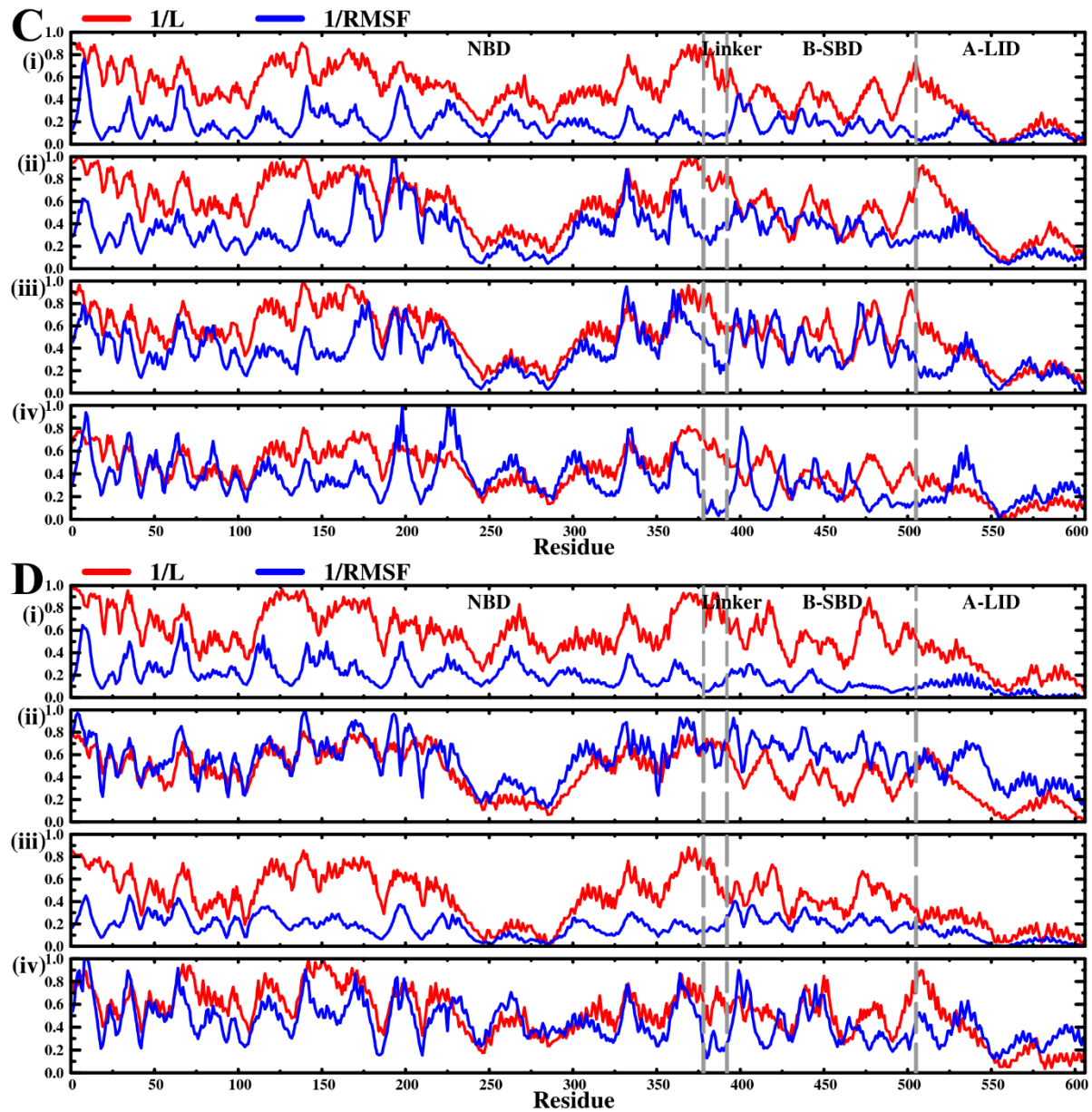


98

99 **Figure S8: A graphical illustration of correlation between BC, 1/L and 1/RMSF of**
100 **duplicate simulation results.** A: (i) Hsp72 apo run2, (ii) Hsp72-SANC00132 complex run2,
101 (iii) Hsp72 endo-apo run2, (iv) Hsp72 endo-complex run1, B: (i) Hsc70 apo run2, (ii) Hsc70-
102 SANC00132 complex run2, (iii) Hsc70 endo-apo run2, (iv) Hsc70 endo-complex run2.



103
104



105

106 **Figure S9: Pairwise comparison of correlation between 1/L and 1/RMSF:** A: (i) Hsp72
107 apo run1, (ii) Hsp72-SANC00132 complex run1, (iii) Hsp72 endo-apo run1, (iv) Hsp72
108 endo-complex run2, B: (i) Hsc70 apo run1, (ii) Hsc70-SANC00132 complex run1, (iii)
109 Hsc70 endo-apo run1, (iv) Hsc70 endo-complex run1. C: (i) Hsp72 apo run2, (ii) Hsp72-
110 SANC00132 complex run2, (iii) Hsp72 endo-apo run2, (iv) Hsp72 endo-complex run1, D: (i)
111 Hsc70 apo run2, (ii) Hsc70-SANC00132 complex run2, (iii) Hsc70 endo-apo run2, (iv)
112 Hsc70 endo-complex run2.

113

Protein	NBD (Nucleotide Binding Domain)					SBD (Substrate Binding Domain)				
	L vs RMSF (100ns)	L vs RMSF (last 15ns)	L^{-1} vs BC	RMSF ⁻¹ (100ns) vs BC	RMSF ⁻¹ (last 15ns) vs BC	L vs RMSF (100ns)	L vs RMSF (last 15ns)	L^{-1} vs BC	RMSF ⁻¹ (100ns) vs BC	RMSF ⁻¹ (last 15ns) vs BC
Hsp72 apo Run1	0.52	0.45	0.45	0.18	0.17	0.48	0.62	0.45	0.45	0.41
Hsp72 apo Run2	0.53	0.45	0.58	0.19	0.26	0.67	0.58	0.51	0.21	0.23
Hsp72-SANC00132 Run1	0.51	0.83	0.58	0.18	0.35	0.11	0.78	0.56	0.26	0.46
Hsp72-SANC00132 Run2	0.61	0.74	0.54	0.13	0.31	0.57	0.78	0.61	0.26	0.26
Hsp72 endo-apo Run1	0.54	0.85	0.46	0.17	0.33	0.64	0.79	0.46	0.39	0.34
Hsp72 endo-apoRun2	0.67	0.83	0.48	0.25	0.31	0.49	0.72	0.55	0.47	0.29
Hsp72 endo-complex Run1	0.59	0.39	0.56	0.38	0.28	0.50	0.14	0.56	0.53	0.00
Hsp72 endo-complex Run2	0.62	0.61	0.56	0.22	0.34	0.50	0.68	0.55	0.19	0.34
Hsc70 apo Run1	0.45	0.84	0.56	0.12	0.43	0.65	0.88	0.54	0.16	0.43
Hsc70 apo Run2	0.42	0.41	0.70	0.12	0.23	0.80	0.72	0.55	0.41	0.37
Hsc70-SANC00132 Run1	0.88	0.88	0.40	0.34	0.33	0.54	0.68	0.45	0.40	0.39
Hsc70-SANC00132 Run2	0.82	0.82	0.43	0.30	0.39	0.53	0.73	0.54	0.06	0.31
Hsc70 endo-apo Run1	0.57	0.59	0.55	0.10	0.38	0.74	0.76	0.53	0.24	0.29
Hsc70 endo-apo Run2	0.68	0.76	0.42	0.27	0.29	0.85	0.90	0.52	0.50	0.41
Hsc70 endo-complex Run1	0.45	0.64	0.54	0.11	0.27	0.73	0.80	0.51	0.35	0.24
Hsc70 endo-complex Run2	0.50	0.59	0.62	0.08	0.38	0.31	0.53	0.46	0.13	0.36

Table S10: Tabulated summary of Pearson's correlation coefficient values calculated domain-wise. The following values were recorded on average: **NBD:** Average L vs RMSF (100ns): $r = 0.59$, L vs RMSF (last 15ns): $r=0.67$, L^{-1} vs BC: $r =0.53$, RMSF⁻¹ (100ns) vs BC: $r =0.20$, RMSF⁻¹ (last 15ns) vs BC: $r = 0.32$. **SBD:** Average L vs RMSF (100ns): $r = 0.57$, L vs RMSF (last 15ns): $r = 0.69$, L^{-1} vs BC: $r = 0.52$, RMSF⁻¹ (100ns) vs BC: $r = 0.32$.

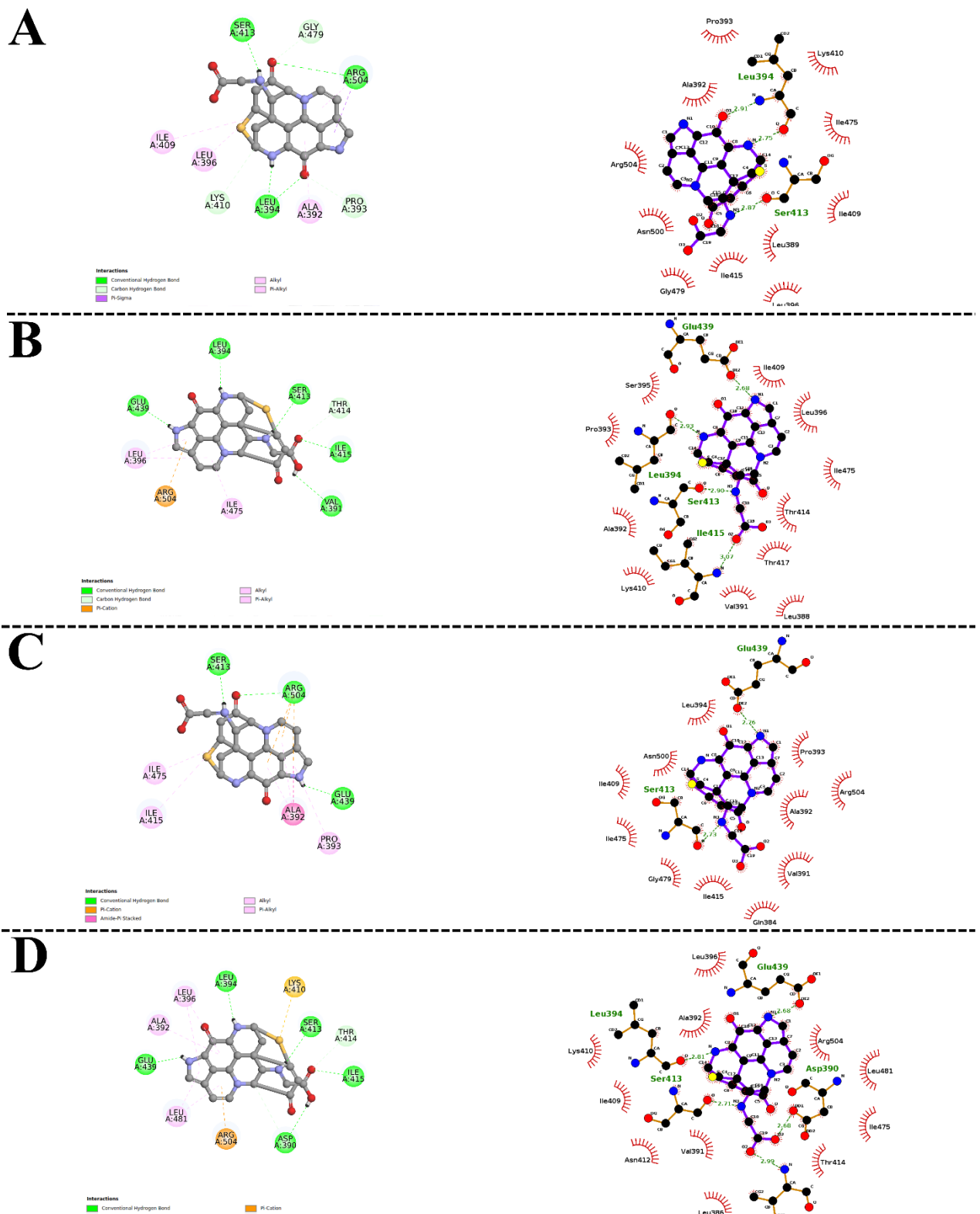
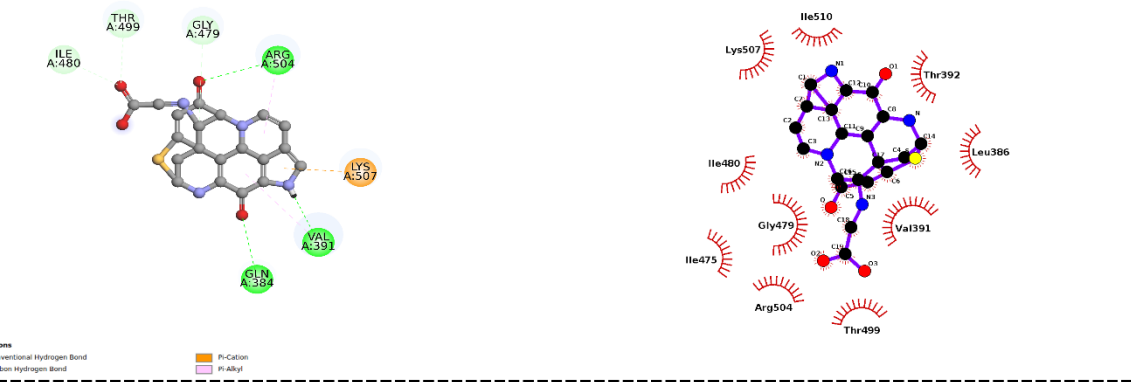
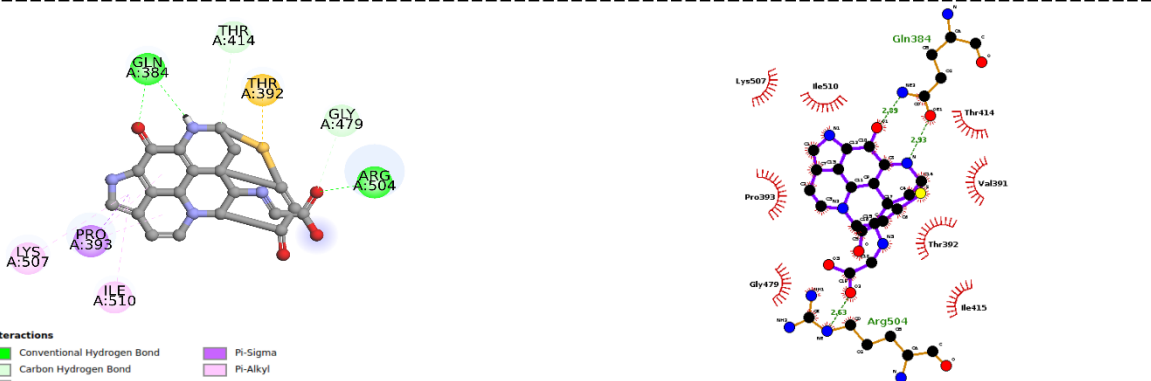


Figure S10: Post MD simulation results: Hsp72-SANC00132 molecular interactions visualised using Discovery studio and LigPlot+. (A) Hsp72-SANC00132 run1, (B) Hsp72-SANC00132 run2, (C) Hsp72 endo-complex run1, (D) Hsp72 endo-complex run2.

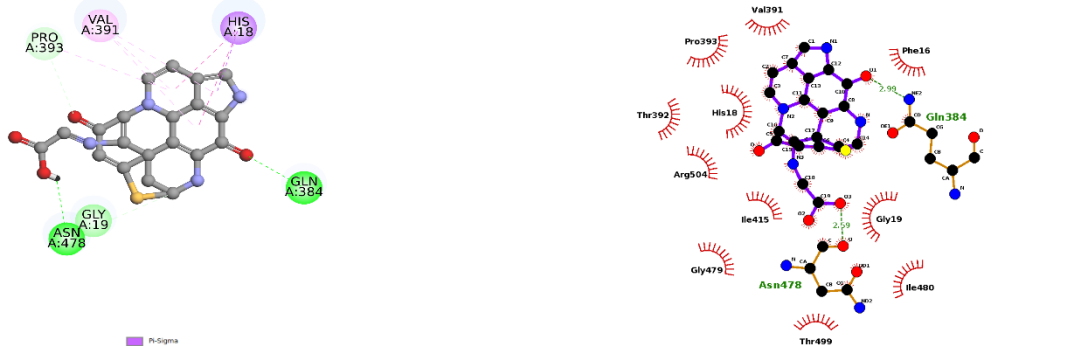
A



B



C



D



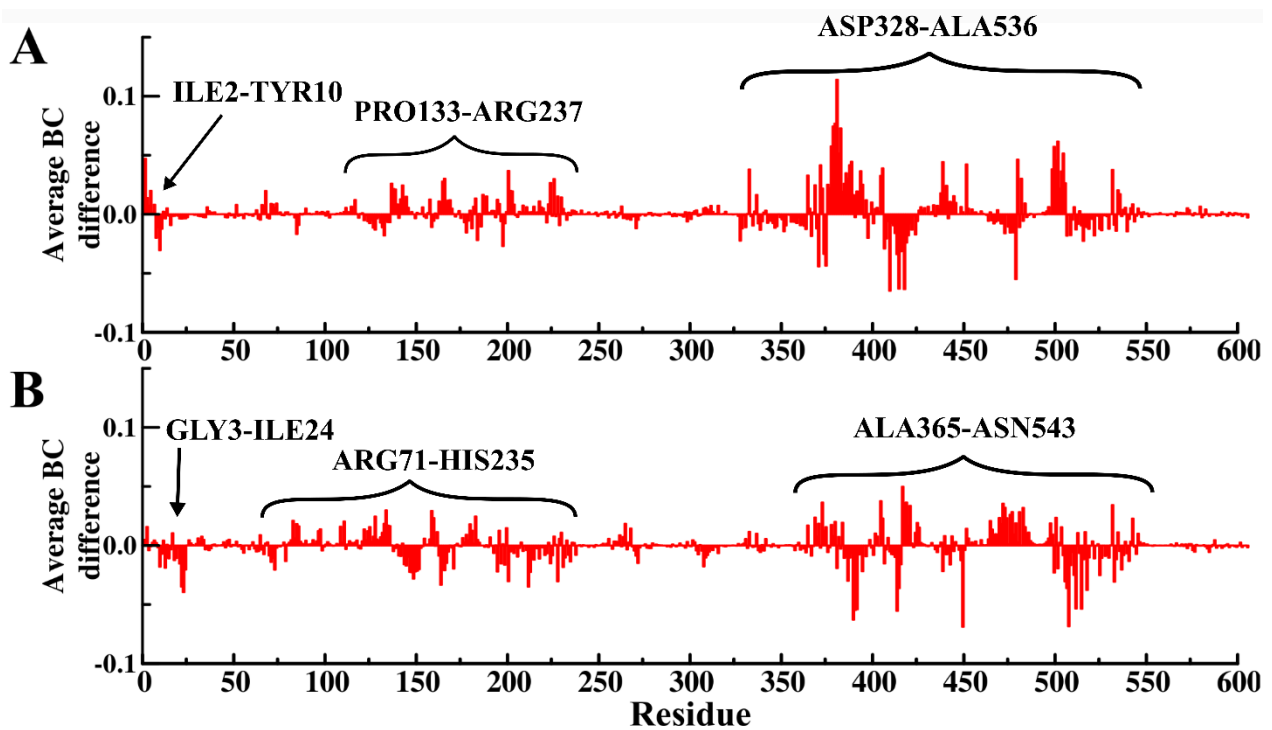
119 **Figure S11: Post MD simulation results. Hsc70-SANC00132 molecular interactions**
120 **visualised by Discovery studio and LigPlot+.** (A) Hsc70-SANC00132 complex run1,
121 (B) Hsc70-SANC00132 complex run2, (C) Hsc70 endo-complex run1, (D) Hsc70 endo-complex
122 run2.

123 **Table S11: Tabulated summary of Hsp72 and Hsc70 residues interacting with SANC00132.**
 124 Residues matching putative allosteric hotspots identified from BC, L and DnaK were noted.
 125 Equivalent amino acid numbering based on the full-length protein sequence was also noted.

126

Protein	Interacting residues	Putative allosteric residue match (L)	Putative allosteric residue match	Corresponding putative allosteric residue match (in DnaK)	Full-length sequence equivalent
Hsp72	ALA392	-	Yes	THR395 [1]	ALA397
	PRO393	-	Yes	PRO396 [2]	PRO398
	LEU394	-	-	LEU397 [2,3]	LEU399
	LEU396	-	-	LEU393 [2]	LEU401
	ILE409	-	-	ILE412 [2]	ILE414
	LYS410	-	-	ALA413 [2]	LYS415
	SER413	-	-	-	SER418
	ILE415	-	-	-	ILE420
	ILE475	-	-	ILE478 [2]	ILE480
	ARG504	Yes	-	-	ARG509
Hsc70	GLN384	Yes	Yes	-	GLN389
	VAL391	-	-	VAL394 [1,3]	VAL396
	THR392	-	-	-	THR397
	PRO393	-	-	PRO396 [2]	PRO398
	ILE415	-	Yes	-	ILE420
	GLY479	Yes	Yes	-	GLY484
	ILE480	Yes	-	-	ILE485
	THR499	-	-	THR502 [2]	THR504
	ARG504	-	-	-	ARG504

127



128

129 **Figure S12: Bar plots displaying protein regions that yielded significant changes in average**
 130 **betweenness centrality values because of ligand binding.** Values were obtained by calculating
 131 SANC00132-free less SANC00132-bound residue centrality on average. A: Hsp72, B: Hsc70.

132

133 **Table S12: Tabulated results of residues showing significant changes in average**
 134 **betweenness centrality.** Residue numbering is according to *E. coli* DnaK sequence (UniProtKB
 135 ID: P0A6Y8). Residues were identified using cutoff values of twice the standard deviation.

136

Protein	Change	Residues
Hsp72	Positive change (Decreased residue centrality)	ILE2, ARG166, ALA365, ALA372, ASP378, LYS379, SER380, GLU381, ASN382, VAL383, LEU386, LEU387, LEU388, LEU389, LEU394, MET405, THR406, GLU439, GLY452, ILE480, ASN482, THR499, ASN500, ASP501, LYS502, ARG504, LEU505, SER532
	Negative change (Increased residue centrality)	TYR10, GLN371, ILE374, LEU375, LYS410, THR414, ILE415, PRO416, LYS418, GLY479
Hsc70	Positive change (Decreased residue centrality)	VAL134, ILE159, ALA373, MET405, THR417, GLN419, GLN421, THR472, PHE473, ASP476, ALA477, LEU481, VAL483, SER532
	Negative change (Increased residue centrality)	GLU22, ILE23, GLN149, VAL164, ASP201, PHE212, PHE228, LEU387, ASP390, VAL391, THR392, THR414, ILE415, LEU450, SER506, LYS507, GLU508, ARG512, GLN515, GLU518, SER533

137

138

139 **Video S1: An accelerated video of 100ns simulation of Hsp72 apo (run1):** The protein is
140 represented as a tube.

141 **Video S2: An accelerated video of 100ns simulation of Hsp72-SANC00132 complex (run1):**
142 The protein is represented as a tube, whereas SANC00132 is depicted in licorice representation.

143 **Video S3: An accelerated video of 100ns simulation of Hsp72 endo-apo run1 (run1):** The
144 protein is represented as a tube, whereas ADP (red) and peptide substrate (green) are shown by
145 licorice representation.

146 **Video S4: An accelerated video of 100ns simulation of Hsp72 endo-complex (run2):** The
147 protein is represented as a tube, whereas ADP (red), SANC00132 (blue), and peptide substrate
148 (green) are shown by licorice representation.

149

150 **REFERENCE**

- 151 1. English, C.A.; Sherman, W.; Meng, W.; Giersch, L.M. The Hsp70 interdomain linker is a
152 dynamic switch that enables allosteric communication between two structured domains. *J.*
153 *Biol. Chem.* **2017**, *292*, 14765–14774, doi:10.1074/jbc.M117.789313.
- 154 2. Penkler, D.; Sensoy, Ö.; Atilgan, C.; Tastan Bishop, Ö. Perturbation-Response Scanning
155 Reveals Key Residues for Allosteric Control in Hsp70. *J. Chem. Inf. Model.* **2017**, *57*,
156 1359–1374, doi:10.1021/acs.jcim.6b00775.
- 157 3. Qi, R.; Sarbeng, E.B.; Liu, Q.; Le, K.Q.; Xu, X.; Xu, H.; Yang, J.; Wong, J.L.; Vorvis, C.;
158 Hendrickson, W.A.; et al. Allosteric opening of the polypeptide-binding site when an
159 Hsp70 binds ATP. *Nat. Struct. Mol. Biol.* **2013**, *20*, 900–7, doi:10.1038/nsmb.2583.

160